ACS APPLIED MATERIALS & INTERFACES

Research Article

www.acsami.org

Efficient Zinc Phthalocyanine/C_{60} Heterojunction Photovoltaic Devices Employing Tetracene Anode Interfacial Layers

Tyler B. Fleetham,[†] John P. Mudrick,[‡] Weiran Cao,[‡] Kody Klimes,[†] Jiangeng Xue,[‡] and Jian Li*[,†]

[†]Department of Material Science and Engineering, Arizona State University, Tempe, Arizona 85284, United States

[‡]Department of Material Science and Engineering, University of Florida, Gainesville, Florida 32611, United States

ABSTRACT: We report the development of efficient small molecular organic photovoltaic devices incorporating tetracene anode interfacial layers. Planar heterojunction devices employing the tetracene anode interfacial layer achieved an EQE enhancement of 150% in the spectral region corresponding to ZnPc absorption. We demonstrate that this enhancement is due to the combined effect of the tetracene layer providing exciton-blocking at the anode/donor interface and potentially an increase in the exciton diffusion length in the ZnPc layer due to increased crystallinity and more preferred molecular stacking orientation. A power conversion efficiency of 4.7% was achieved for a planar heterojunction of a modified zinc phthalocyanine based material and C_{60} when employing the tetracene anode interfacial layer. By utilizing a planar-mixed heterojunction structure a peak EQE of nearly 70% and a power conversion efficiency of 5.8% was achieved.

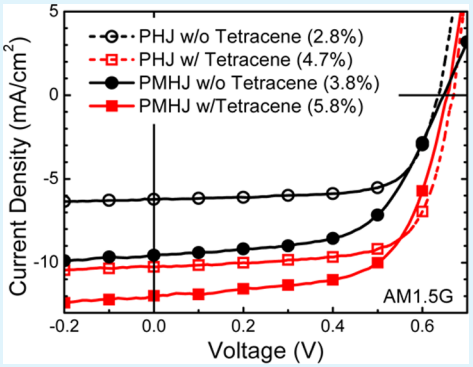

KEYWORDS: *organic photovoltaics, small molecule, morphology, exciton blocker, planar-mixed heterojunction*

INTRODUCTION

Organic photovoltaic devices (OPVs) have remained a research topic of great interest over the past two decades because of steady advances in the physical understanding of organic electronic materials and devices, continual increases in device efficiencies and stability, and growing commercialization of the field.[1−3] Devices employing conjugated polymers have received the most attention because of the simplicity of their solution-processable bulk heterojunction structure and power conversion efficiencies which have steadily increased and exceeded 10% most recently.[4−8] Nevertheless, small molecule organic semiconductors have their own advantages of more uniform material properties with higher purity and the ease of preparing multilayer structures in vacuum to precisely control the carrier and exciton dynamics inside devices.[9−11] Much of the current efforts on small molecule OPVs have focused on developing new materials for either high open circuit voltage (V_{OC}) or to extend the absorption into the near-infrared range (NIR) with materials such as subphthalocyanine (SubPc),[12] tetrephenyldibenzoperiflanthene (DBP),[13] squarine dyes,[14] merocyanine dyes,[15] or Ir complexes.[16] However, synthesis of many of these materials can be challenging and the improvements often come at the expense of other performance parameters, such as fill factor in the case of SubPc, or V_{OC} in the case of many NIR absorbers. Thus, further development of these classes of materials as well as the application of new device structures is crucial.

Among the various classes of small molecular absorbers, metal phthalocyanines have received much of the attention due to their strong absorption, their high thermal and electrochemical stability, as well as their well-established, inexpensive synthetic production in bulk quantities.[17] Nevertheless, the low exciton diffusion lengths and low open-circuit voltage (V_{OC}) of metal phthalocyanines significantly limits their efficiencies in OPVs.[18,19] Recently, phthalocyanine based OPVs, as well as a number of other material systems, have seen moderate enhancement in OPV performance with the addition anode interfacial layers employing inorganic materials such as metal oxides or organic small molecular materials.[20−29] The origin of the efficiency enhancement from anode interfacial layers is multivariate due to factors such as improving charge extraction, providing exciton or electron blocking, optimizing the optical intensity profile, or modifying the morphology of the overlayers.[29] In this article, we report the application of a tetracene anode interfacial layer to drastically enhance the photovoltaic characteristics of a modified zinc phthalocyanine (ZnPc) material in both planar heterojunction and planar-mixed heterojunction cells with C_{60}. The incorporation of the tetracene layer leads to an approximately 4 mA/cm^2 increase in the short-circuit current density (J_{SC}) for both cells under 1 sun AM1.5G solar illumination, and the power conversion efficiency, η_P, was increased from 2.8 ± 0.2% to 4.7 ± 0.3% for the planar heterojunction cell and from 3.8 ± 0.3% to 5.8 ± 0.3% for the more efficient planar-mixed heterojunction cell.

RESULTS AND DISCUSSION

Typically, ZnPc/C_{60} heterojunctions demonstrate low efficiencies of η_P = 1−2%, due to their low open-circuit voltages of less

Received: January 22, 2014
Accepted: April 7, 2014
Published: April 7, 2014

   dx.doi.org/10.1021/am500472m | ACS Appl. Mater. Interfaces 2014, 6, 7254−7259

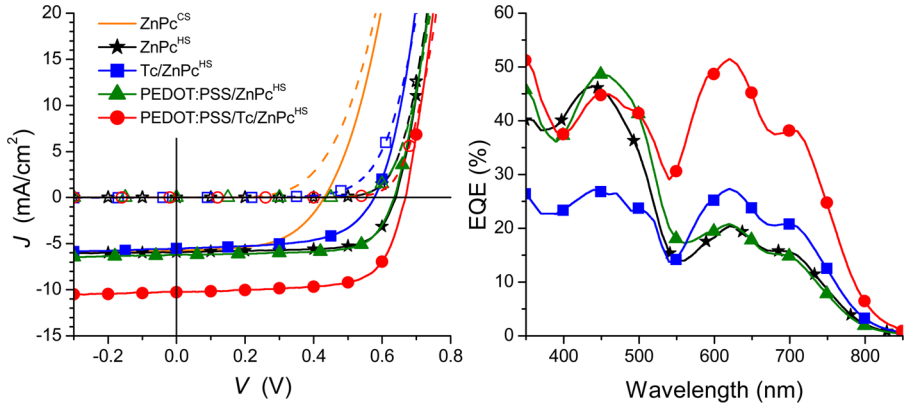

Figure 1. (a) Current density vs voltage ($J-V$) characteristics in the dark (open symbols/dashed lines) and at 1 sun AM1.5G illumination (solid symbols/lines) and (b) external quantum efficiency (EQE) spectra for planar heterojunction devices of $ZnPc^{CS}$ (no symbols), $ZnPc^{HS}$ (stars), and $ZnPc^{HS}$ with the anode interfacial layers: 10 nm tetracene (Tc, circles), PEDOT:PSS (triangles), and PEDOT:PSS/10 nm Tc (squares) in the device structure: ITO/AIL/donor 15 nm/C_{60} 30 nm/PTCDI 10 nm/BCP 14 nm/Al.

than 0.5 V and limited exciton diffusion length of ~10 nm.[18] We recently reported a simple one-step, solvent-free reaction using inexpensive reagents 1,2-dicyanobenzne and zinc chloride to produce partially chlorinated ZnPc (denoted as $ZnPc^{HS}$) at a large scale in high yield.[30] This material demonstrated a significant increase in both the open-circuit voltage and fill factor in ZnPc/C_{60} planar heterojunction photovoltaic cells as compared to a commercially obtained ZnPc (denoted as $ZnPc^{CS}$).[30] The current density−voltage ($J-V$) characteristics of planar heterojunction devices employing these two materials are shown in Figure 1, which have the structure of indium−tin oxide (ITO)/$ZnPc^{CS}$ or $ZnPc^{HS}$ (15 nm)/C_{60} (30 nm)/PTCDI (10 nm)/BCP (14 nm)/Al. Here *N,N′*-dihexyl-perylene-3,4,9,10-bis(dicarboximide) (PTCDI) was employed as an interfacial layer between the C_{60} acceptor and the bathocuproine (BCP) exciton blocking layer in order to facilitate the migration of metal atoms through the BCP layer to improve electron injection.[31,32] From Figure 1a, we see that the two devices have nearly identical short-circuit current densities of approximately 5.8 mA/cm^2 under 1 sun AM1.5G solar illumination, but the open-circuit voltage increases from 0.43 ± 0.01 V to 0.64 ± 0.01 V and the fill factor from 0.55 ± 0.01 to 0.70 ± 0.01 when the commercial ZnPc was replaced by $ZnPc^{HS}$, leading to an overall η_P enhancement from 1.4 ± 0.1% to 2.6 ± 0.1% (also see Table 1).

To improve the efficiency of the $ZnPc^{HS}$ devices, we employed three different interfacial layers between the ITO anode and the $ZnPc^{HS}$ donor layer: a 10 nm thick tetracene (Tc) layer, a poly(3,4-ethylenedioxythiophene) poly-(styrenesulfonate) (PEDOT:PSS) layer, or a PEDOT:PSS/tetracene (10 nm) bilayer. The $J-V$ characteristics of ZnPc (15 nm)/C_{60} (30 nm) planar heterojunction devices with the various interlayers are shown in Figure 1a, and the photovoltaic performance parameters of these devices are summarized in Table 1. When a single PEDOT:PSS layer is used, there is minimal change in the $J-V$ characteristics with only a slight increase in J_{SC} to 6.2 ± 0.3 mA/cm^2. Conversely, a single 20 nm thick Tc interlayer actually leads to noticeable reductions in both J_{SC} and V_{OC}. However, when tetracene is deposited on top of PEDOT:PSS, we observe a dramatic increase in J_{SC} by approximately 4 mA/cm^2 to 10.3 ± 0.5 mA/cm^2. Along with a minor increase in V_{OC} to 0.67 ± 0.01 V and nearly constant fill factor, the power conversion efficiency is increased from 2.8 ± 0.2% to 4.7 ± 0.3%. This is among the highest reported for small molecular planar heterojunction devices and is especially high considering the simplicity of the materials system.[10,11]

Table 1. Photovoltaic Performance Characteristics for ZnPc/C60 Devices

device structure[a]	J_{sc} (mA/cm^2)	V_{oc} (V)	FF	η_{PCE} (%)
$ZnPc^{CS}$ (PHJ)	5.8 ± 0.3	0.43 ± 0.01	0.55 ± 0.01	1.4 ± 0.1
$ZnPc^{HS}$ (PHJ)	5.9 ± 0.3	0.64 ± 0.01	0.70 ± 0.01	2.6 ± 0.1
PEDOT:PSS/ $ZnPc^{HS}$ (PHJ)	6.2 ± 0.3	0.64 ± 0.01	0.68 ± 0.02	2.8 ± 0.2
tetracene/$ZnPc^{HS}$ (PHJ)	5.5 ± 0.3	0.58 ± 0.01	0.58 ± 0.03	1.9 ± 0.3
PEDOT:PSS/ tetracene/$ZnPc^{HS}$ (PHJ)	10.3 ± 0.5	0.67 ± 0.01	0.69 ± 0.01	4.7 ± 0.3
PEDOT:PSS/ $ZnPc^{HS}$ (PMHJ)	10.0 ± 0.5	0.65 ± 0.01	0.59 ± 0.03	3.8 ± 0.3
PEDOT:PSS/ tetracene/$ZnPc^{HS}$ (PMHJ)	13.9 ± 0.5	0.66 ± 0.01	0.63 ± 0.03	5.8 ± 0.3

[a]PHJ devices have an active region of $ZnPc^{CS}$ or $ZnPc^{HS}$/C60 (15 nm/30 nm). PMHJ devices have an active region of $ZnPc^{HS}$(15 nm)/$ZnPc^{HS}$:C60 (2:1, 20 nm)/C60 (30 nm).

The external quantum efficiency (EQE) spectra of these $ZnPc^{HS}/C_{60}$ planar heterojunction devices with various interfacial layers are shown in Figure 1b. The EQE spectra for devices without any anode interfacial layer or with a single PEDOT:PSS layer showed very similar shape and magnitude. When a single Tc layer is employed, the EQE spectrum shows an enhancement in the region where ZnPc absorption dominates (λ = 550 to 800 nm) from a maximum of 21% to 27%, although that is compensated by a significant reduction of EQE at λ < 550 nm where C_{60} absorption dominates. However, when the PEDOT:PSS/Tc dual layer is used, the high EQE below 550 nm is mostly restored, and a much stronger enhancement in EQE in the ZnPc absorption region is observed. The peak EQE at λ = 620 nm increases from 21 to 52%, a relative increase of approximately 150%. The minimal decrease in EQE at λ < 500 nm is most likely due to absorption in the Tc layer since, by comparing the absorption spectra (Figure 2) to the EQE for the tetracene-containing devices, we conclude that absorption in Tc (λ = 400 to 550 nm) does not contribute to the photocurrent.

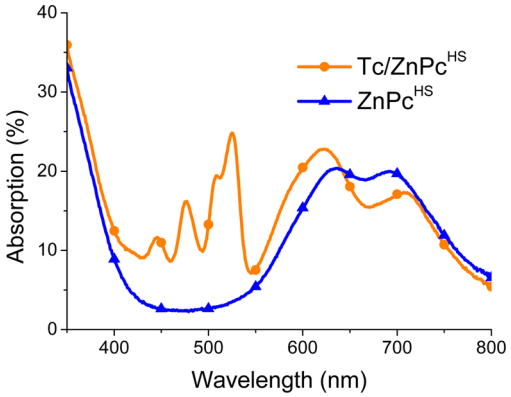

Figure 2. Thin film absorption spectra for glass/ITO/PEDOT:PSS/ZnPc^{HS} (triangles) and for glass/ITO/PEDOT:PSS/tetracene (10 nm)/ZnPc^{HS} (15 nm) (circles).

The thin film absorption for the multilayer stack of glass/ITO/PEDOT:PSS/Tc (0 or 10 nm)/ZnPc^{HS} (15 nm) determined from reflection and transmission measurements using a UV Cary 5000 spectrophotometer equipped with an integration sphere is shown in Figure 2. Upon comparing the absorption spectra of the ZnPc^{HS} films with or without the Tc layer, it is apparent that the large increase in EQE in the ZnPc^{HS} spectrum is not a result of an increase in absorption. There is, however, a significant change in the shape of the ZnPc^{HS} absorption spectrum when the Tc layer is included as the intensity ratio of the peak centered at λ = 610 to 620 nm to the peak at $\lambda \approx$ 700 nm becomes significantly higher, along with the appearance of a noticeable shoulder at $\lambda \approx$ 580 nm. This has been previously attributed to an increase in the concentration of dimer and higher-order aggregates,[33] suggesting an increase in crystallinity when the ZnPc^{HS} is deposited on Tc (on PEDOT:PSS).

To examine the morphology change, we collected X-ray diffraction (XRD) patterns of ZnPc^{HS} on the various interfacial layers in the θ–2θ mode and show them in Figure 3. Without

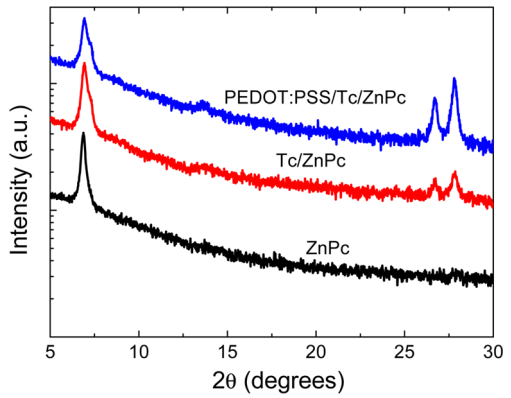

Figure 3. X-ray diffraction patterns of 150 nm ZnPc films, with or without interlayers, grown on Si substrates coated with a thermal SiO_2 layer.

either PEDOT:PSS or Tc, ZnPc^{HS} has a single diffraction peak centered at 2θ = 6.9°, corresponding to a 12.7 Å interplanar spacing which has been attributed to the (200) molecular plane of the α phase of ZnPc with edge-on orientation on the substrate.[34] For the ZnPc^{HS} films grown on tetracene and PEDOT:PSS/Tc, this feature evolves into a doublet with peaks at 6.9 and 7.3°, the latter peak corresponding to the (001) plane of the highly crystalline Tc layer.[35] In addition to the (200) α-ZnPc diffraction peak, the film grown on PEDOT:PSS/Tc interfacial layers shows a weak feature centered at 13.6°, which although not very conclusive, corresponds to the higher order (400) diffraction of α-ZnPc, again suggesting improved crystallinity in this ZnPc^{HS} film. A pair of peaks at 2θ = 26.7 and 27.8° are present in ZnPc films deposited on top of Tc and PEDOT:PSS/Tc, which agree with the $(0\bar{1}2)$ and $(\bar{1}12)$ diffractions of the triclinic α-ZnPc phase, respectively.[36] These high angle diffraction peaks correspond to interplanar spacings of 3.2 to 3.3 Å, which is close to the interplanar distance in ZnPc crystals along the molecular stacking direction. Given the geometry of the θ–2θ mode of XRD measurements, this suggests that the Tc interfacial layer, especially with an additional underlying PEDOT:PSS layer, promotes the growth of ZnPc molecules in the "face-on" orientation such that the molecular stacking direction is mostly normal to the substrate surface. From the device and thin film characterization, we attribute the EQE increase in the donor absorption region to an increase in exciton diffusion efficiency, likely through a combination of multiple factors. The tetracene layer, which has a wider optical gap than ZnPc (see Figure 2), serves as an exciton blocking layer at the anode interface, thus preventing the quenching of photogenerated excitons in the ZnPc layer by the anode. The tetracene layer increases the crystallinity of the donor layer, which has been correlated to an increase in the exciton diffusion length.[37] Moreover, as revealed by the XRD results, the orientation of ZnPc molecules was changed from mostly edge-on without the tetracene layer to a mixture of edge-on and face-on with the tetracene layer. The face-on configuration suggests that the molecular π–π stacking direction is in the film thickness direction, thus further promoting the exciton diffusion process toward the donor–acceptor interface. For the devices without the PEDOT:PSS layer, the incomplete coverage of Tc on ITO results in direct contact of ZnPc with ITO in certain areas, leading to incomplete exciton confinement and therefore lower photocurrent. More experimental effort will be needed to clarify which effects lead to the high exciton diffusion efficiency and consequently high external quantum efficiency in the devices with the anode interlayers.

To further increase the efficiency of these devices, planar-mixed heterojunction devices were fabricated by adding an additional 20 nm thick ZnPc:C_{60} mixed layer in between the neat donor and acceptor layers. Planar-mixed heterojunctions have been used previously to circumvent the trade-off between the thin films needed for efficient exciton diffusion and the thick films needed for complete absorption, allowing simultaneous optimization of both absorption and internal quantum efficiency.[38−40] Devices were fabricated with the structure: ITO/PEDOT:PSS/Tc (0 or 10 nm)/ZnPc^{HS} (15 nm)/ZnPc^{HS}:C_{60} (20 nm, 2:1 by weight)/C_{60} (30 nm)/PTCDI (10 nm)/BCP (14 nm)/Al. As seen in Figure 4a as well as in Table 1, a significant increase in J_{SC} from 10.0 ± 0.5 mA/cm^2 to 13.9 ± 0.5 mA/cm^2 was obtained when the Tc anode interfacial layer was included, which was accompanied by a nearly identical V_{OC} and a slight increase in FF from 0.59 to 0.63. The external quantum efficiency in Figure 4b shows that the enhancement is again mainly attributed to enhanced contribution from absorption by the ZnPc^{HS} layer. The maximum EQE of the Tc-containing device approaches 70% at λ = 620 nm, whereas it was below 50% for the device without the Tc

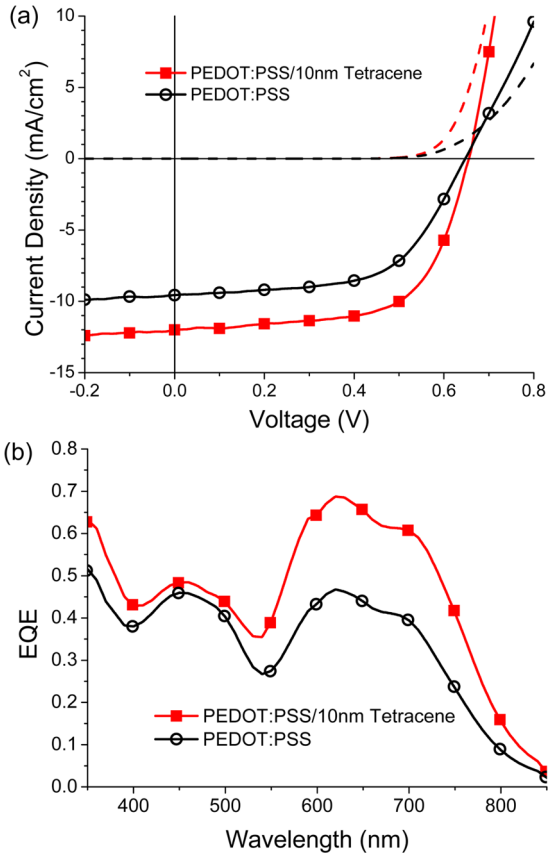

Figure 4. (a) Current density vs voltage (J–V) characteristics and (b) external quantum efficiency vs wavelength for planar-mixed heterojunction devices of $ZnPc^{HS}$ with the anode interfacial layers PEDOT:PSS (black circles) and PEDOT:PSS/10 nm tetracene (red squares) in the device structure: ITO/AIL/$ZnPc^{HS}$ 15 nm/$ZnPc^{HS}$:C_{60} 20 nm (2:1 by weight)/C_{60} 30 nm/PTCDI 10 nm/BCP 14 nm/Al.

layer. The net increase in J_{SC} of 3.9 mA/cm^2 is approximately the same as that for the planar heterojunction devices (4.1 mA/cm^2), which further supports our conclusion above that the photocurrent increase is mainly due to improved exciton diffusion efficiency in the neat ZnPc layer. Furthermore, the slightly higher fill factor for the planar-mixed heterojunction device with the Tc layer tends to indicate that the creation of larger, more crystalline ZnPc domains in the neat layer may aid the formation of a more structured interpenetrating network in the mixed layer which will enhance both the fill factor and the short circuit current. As a result, the inclusion of the Tc anode interfacial layer improves the power conversion efficiency of the ZnPc:C_{60} planar-mixed heterojunction devices from η_P = 3.8 ± 0.3% to 5.8 ± 0.3%, among the highest achieved to date for single donor–acceptor heterojunction (i.e., nontandem) devices based on this material system and among the highest small molecule-based nontandem OPV devices.[41−43]

In summary, we demonstrated the effect of using a tetracene anode interfacial layer on the efficiency of organic photovoltaic cells based on a home-synthesized ZnPc. Planar heterojunction devices employing the tetracene anode interfacial layer achieved an EQE enhancement of 150% in the spectral region corresponding to ZnPc absorption. This was mainly attributed to the enhancement in exciton diffusion efficiency, with the tetracene layer providing exciton-blocking function at the anode/donor interface and increasing the exciton diffusion length in the ZnPc layer due to increased crystallinity and more preferred molecular orientation/stacking. The enhancement from tetracene anode interfacial layers is not limited to $ZnPc^{HS}$ and is expected to be observed for a variety of material systems provided the HOMO and LUMO levels of the donor material are compatible with those of the tetracene (i.e., prevent dissociation and block excitons).[44] Applying these principles to a planar-mixed heterojunction ultimately yielded a η_P of 5.8 ± 0.3% and a peak EQE of nearly 70%. Further application of state-of-the-art donor and acceptor materials as well as integration of light trapping structures,[45] tandem devices,[1,38] or other architectures will likely further increase the efficiencies of these devices and 1 day may contribute to the development of commercial production of OPV devices.[1]

EXPERIMENTAL SECTION

$ZnPc^{HS}$ Synthesis. Zinc chloride was mixed thoroughly with an excess of 1,2-dicyanobenzene in a 1:10 ratio in a round-bottom flask. The reactants were quickly heated to 200 °C and refluxed for 6 h to yield a dark blue-violet solid product. The crude product was cooled to room temperature, washed with dichloromethane, and filtered to wash out the soluble impurities and remaining starting materials. The solid filtrate product was dried thoroughly then sublimed in a four-zone thermal gradient furnace for 12 h with the first two zones at 420 °C, a middle zone of 380 °C, and the cool zone at 340 °C under pressures of 1 × 10^{-6} Torr. After cooling to room temperature the metallic violet purified crystals were collected from the middle temperature zone.

Materials. The commercial ZnPc and tetracene were both purchased from Sigma-Aldrich (99% purity), C_{60} was purchased from MER Corp., PEDOT:PSS (Clevios AI4083) was purchased from Baytron AG, and bathocuproine was purchased from TCI Corp. PTCDI was synthesized following the literature.[13] All materials were purified one to two times using the thermal gradient sublimation method prior to use for thin film deposition and device fabrication.

Device Fabrication. OPV devices were fabricated on glass substrates precoated with a patterned transparent indium tin oxide (ITO) anode (sheet resistance ∼15 Ω/□). Prior to organic material deposition, the ITO substrates were cleaned by subsequent sonication in deionized water, acetone, and isopropanol followed by a 15 min UV-ozone treatment. PEDOT:PSS was filtered through a 0.45 μm filter, spun coat at 5000 rpm for 60 s, then baked at 180 °C for 30 min yielding an approximately 40 nm thick films. The organic and cathode materials were deposited by high vacuum thermal evaporation at a base pressure of about 1 × 10^{-7} Torr. The film thickness was monitored by quartz crystal microbalances, and typical deposition rates were 0.5 to 1.5 Å/s for organic materials and 1 to 2 Å/s for the Al cathode. The patterned electrodes formed device areas of 4 mm^2 in cross-bar geometry, and 16 devices with identical structures were fabricated in each batch.

Characterization. Current–voltage (I–V) characteristics in the dark and under illumination were measured using a Keithley 4200 semiconductor characterization system. Illumination was provided by a Newport 150 W Xe-arc solar simulator outfitted with an AM1.5G filter and neutral density filters. The light intensity was determined using a Hamamatsu Si reference cell (Model C24 S1787–04) calibrated by National Renewable Energy Laboratory (NREL). To measure the external quantum efficiency (EQE) as a function of wavelength, a monochromatic beam of light was generated by using a Xe lamp (Optronic Laboratories) in conjunction with an Optronic Lab OL750 spectroradiometer. The monochromatic beam intensity was measured using a calibrated Newport Si photodetector. Spectral mismatch between the solar simulator and the standard AM1.5G solar spectrum is calculated according to the ASTM Standard E973[46] and used to adjust the solar simulator intensity to yield 1 sun (100 mW/cm^2) for the test cell, such that integrating the measured EQE spectrum with the standard 1 sun AM1.5G solar spectrum yields a short-circuit current density typically within 5% of the experimental result.

Thin films of glass/ITO/(PEDOT:PSS)/Tc(0 or 20 nm)/$ZnPc^{HS}$ (15 nm) were also deposited for absorption and atomic force

microscopy (AFM) measurements. Absorption was from reflection and transmission measurements determined using a UV Cary 500 spectrometer equipped with an integration sphere where % absorption = 100 − % reflection − % transmission. Atomic force microscopy was carried out using a Park XE-150 AFM in a noncontact mode. X-ray diffraction (XRD) patterns of the organic films were obtained using a Philips X'pert MRD diffractometer in the $\theta-2\theta$ geometry with a Cu K_α radiation source.

AUTHOR INFORMATION

Corresponding Author

*E-mail: jian.li.1@asu.edu.

Notes

The authors declare no competing financial interest.

ACKNOWLEDGMENTS

The authors thank the National Science Foundation (CHE-0748867), the Advanced Photovoltaics Center at Arizona State University, the Research Corporation for Science Advancement, and the University of Florida Office of Research for partial support of this work.

REFERENCES

(1) Peumans, P.; Yakimov, A.; Forrest, S. R. Small Molecular Weight Organic Thin-Film Photodetectors and Solar Cells. *J. Appl. Phys.* **2003**, *93*, 3693−3723.

(2) Dennler, G.; Scharber, M. C.; Brabec, C. J. Polymer-Fullerene Bulk-Heterojunction Solar Cells. *Adv. Mater.* **2009**, *21*, 1323−1338.

(3) Heremans, P.; Cheyns, D.; Rand, B. P. Strategies for Increasing the Efficiency of Heterojunction Organic Solar Cells: Material Selection and Device Architecture. *Acc. Chem. Res.* **2009**, *42*, 1740−1747.

(4) Li, G.; Zhu, R.; Yang, Y. Polymer Solar Cells. *Nat. Photonics* **2012**, *6*, 153−161.

(5) He, Z.; Zhong, C.; Su, S.; Xu, M.; Wu, H.; Cao, Y. Enhanced Power-Conversion Efficiency in Polymer Solar Cells Using an Inverted Device Structure. *Nat. Photonics* **2012**, *6*, 591−595.

(6) Li, W.; Furlan, A.; Hendriks, K. H.; Wienk, M. M.; Janssen, R. A. Efficient Tandem and Triple-Junction Polymer Solar Cells. *J. Am. Chem. Soc.* **2013**, *135*, 5529−5532.

(7) You, J.; Dou, L.; Yoshimura, K.; Kato, T.; Ohya, K.; Moriarty, T.; Emery, K.; Chen, C.-C.; Gao, J.; Li, G.; Yang, Y. A Polymer Tandem Solar Cell with 10.6% Power Conversion Efficiency. *Nat. Commun.* **2013**, *4*, 1466.

(8) Green, M. A.; Emery, K.; Hishikawa, Y.; Warta, W.; Dunlop, E. D. Solar Cell Efficiency Tables (Version 42). *Prog. Photovolt.* **2013**, *21*, 827−837.

(9) Xue, J. Perspectives on Organic Photovoltaics. *Polym. Rev.* **2010**, *50*, 411−419.

(10) Mishra, A.; Bäuerle, P. Small Molecule Organic Semiconductors on the Move: Promises for Future Solar Energy Technology. *Angew. Chem., Int. Ed.* **2012**, *51*, 2020−2067.

(11) Lin, Y.; Li, Y.; Zhan, X. Small Molecule Semiconductors for High-Efficiency Organic Photovoltaics. *Chem. Soc. Rev.* **2012**, *41*, 4245−4272.

(12) Mutolo, K. L.; Mayo, E. I.; Rand, B. P.; Forrest, S. R.; Thompson, M. E. Enhanced Open-Circuit Voltage in Subphthalocyanine/C60 Organic Photovoltaic Cells. *J. Am. Chem. Soc.* **2006**, *128*, 8108−8109.

(13) Wagner, J.; Gruber, M.; Hinderhofer, A.; Wilke, A.; Bröker, B.; Frisch, Jo.; Amsalem, P.; Vollmer, A.; Opitz, A.; Koch, N.; Schreiber, F.; Brütting, W. High Fill Factor and Open Circuit Voltage in Organic Photovoltaic Cells with Diindenoperylene as Donor Material. *Adv. Funct. Mater.* **2010**, *20*, 4295−4303.

(14) Wei, G.; Xiao, X.; Wang, S.; Sun, K.; Bergemann, K. J.; Thompson, M. E.; Forrest, S. R. Functionalized Squaraine Donors for Nanocrystalline Organic Photovoltaics. *ACS Nano* **2012**, *6*, 972−978.

(15) Steinmann, V.; Kronenberg, N. M.; Lenze, M. R.; Graf, S. M.; Hertel, D.; Meerholz, K.; Bürckstümmer, H.; Tulyakova, E. V.; Würthner, F. Simple, Highly Efficient Vacuum-Processed Bulk Heterojunction Solar Cells Based on Merocyanine Dyes. *Adv. Energy Mater.* **2011**, *1*, 888−893.

(16) Fleetham, T. B.; Wang, Z.; Li, J. Exploring Cyclometalated Ir Complexes as Donor Materials for Organic Solar Cells. *Inorg. Chem.* **2013**, *52*, 7338−7343.

(17) Zheng, Y.; Xue, J. Organic Photovoltaic Cells Based on Molecular Donor-Acceptor Heterojunctions. *Polym. Rev.* **2010**, *50*, 420−453.

(18) Kim, I.; Haverinen, H. M.; Wang, Z.; Madakuni, S.; Kim, Y.; Li, J.; Jabbour, G. E. Efficient Organic Solar Cells Based on Planar Metallophthalocyanines. *Chem. Mater.* **2009**, *21*, 4256−4260.

(19) Xue, J.; Uchida, S.; Rand, B. P.; Forrest, S. R. 4.2% Efficient Organic Photovoltaic Cells with Low Series Resistances. *Appl. Phys. Lett.* **2004**, *84*, 3013−3015.

(20) Ma, H.; Yap, H.-L.; Huang, F.; Jen, A. K-Y. Interface Engineering for Organic Electronics. *Adv. Funct. Mater.* **2010**, *20*, 1371−1388.

(21) Chen, S.; Manders, J. R.; Tsang, S.-W.; So, F. Metal Oxides for Interface Engineering in Polymer Solar Cells. *J. Mater. Chem.* **2012**, *22*, 24202−24212.

(22) Savva, A.; Petraki, F.; Elefteriou, P.; Sygellou, L.; Voigt, M.; Giannouli, M.; Kennou, S.; Nelson, J.; Bradley, D. D. C.; Brabec, C. J.; Choulis, S. A. The Effect of Organic and Metal Oxide Interfacial layers on the Performance of Inverted Organic Photovoltaics. *Adv. Energy Mater.* **2013**, *3*, 391−398.

(23) Irwin, M. D.; Buchholz, D. B.; Hains, A. W.; Chang, R. P. H.; Marks, T. J. p-Type Semiconducting Nickel Oxide as an Efficiency-Enhancing Anode Interfacial Layer in Polymer Bulk-heterojunction Solar Cells. *Proc. Nat. Acad. Sci. U.S.A.* **2008**, *105*, 2783−2787.

(24) Cheng, C. H.; Wang, J.; Du, G. T.; Shi, S. H.; Du, Z. J.; Fan, Z. Q.; Bian, J. M.; Wang, M. S. Organic Solar Cells with Remarkable Enhanced Efficiency by using a CuI Buffer to Control the Molecular Orientation and Modify the Anode. *Appl. Phys. Lett.* **2010**, *97*, 083305.

(25) Yook, K. S.; Chin, B. D.; Lee, J. Y.; Lassiter, B. E.; Forrest, S. R. Vertical Orientation of Copper Phthalocyanine in Organic Solar Cells Using a Small Molecular Weight Organic Templating Layer. *Appl. Phys. Lett.* **2011**, *99*, 043308.

(26) Sullivan, P.; Jones, T. S.; Ferguson, A. J.; Huetz, S. Structural Templating as a Route to Improved Photovoltaic Performance in Copper Phthalocyanine/Fullerene (C_{60}) Heterojunctions. *Appl. Phys. Lett.* **2007**, *91*, 233114.

(27) Yu, B.; Huang, L.; Wang, H.; Yan, D. Efficient Organic Solar Cells Using a High-Quality Crystalline Thin Film as a Donor Layer. *Adv. Mater.* **2010**, *22*, 1017−1020.

(28) Zhao, W.; Mudrick, J. P.; Zheng, Y.; Hammond, W. T.; Yang, Y.; Xue, J. Enhancing Photovoltaic Response of Organic Solar Cells Using a Crystalline Molecular Template. *Org. Electron.* **2012**, *13*, 129−135.

(29) Fleetham, T.; O'Brien, B.; Mudrick, J. P.; Xue, J.; Li, J. External Quantum Efficiency Enhancement in Organic Photovoltaic Devices Employing Dual Organic Anode Interfacial Layers. *Appl. Phys. Lett.* **2013**, *103*, 083303.

(30) Fleetham, T. B.; Bakkan, N.; Mudrick, J. P.; Myers, J. D.; Cassidy, V. D.; Cui, J.; Xue, J.; Li, J. Enhanced Open-Circuit Voltage in Organic Photovoltaic Cells with Partially Chlorinated Zinc Phthalocyanine. *J. Mater. Sci.* **2013**, *48*, 7104−7114.

(31) Peumans, P.; Forrest, S. R. Very-High-Efficiency Double-Heterostructure Copper Phthalocyanine/C60 Photovoltaic Cells. *Appl. Phys. Lett.* **2001**, *79*, 126−128.

(32) Kim, I.; Haverinen, H. M.; Li, J.; Jabbour, G. E. Enhancement of Device Performance of Organic Solar Cells by an Interfacial Perylene Derivative Layer. *Appl. Mater. & Interfaces* **2010**, *2*, 1390−1394.

(33) Rand, B. P.; Xue, J.; Uchida, S.; Forrest, S. R. Mixed Donor-Acceptor Molecular Heterojunctions for Photovoltaic Applications. I. Material Properties. *J. Appl. Phys.* **2005**, *98*, 124902.

(34) Schünemann, C.; Elschner, C.; Levin, A. A.; Levichkova, M.; Leo, K.; Riede, M. Zinc Phthalocyanine — Influence of Substrate

Temperature, Film Thickness, and Kind of Substrate on the Morphology. *Thin Solid Films* **2011**, *519*, 3939−3945.
(35) Abthagir, S.; Ha, Y.-G.; You, E.-A.; Jeong, S.-H.; Seo, H.-S.; Choi, J.-H. Studies of Tetracene- and Pentacene-Based Organic Thin-Film Transistors Fabricated by the Neutral Cluster Beam Deposition Method. *J. Phys. Chem. B* **2005**, *109*, 23918−23924.
(36) Schünemann, C.; Wynands, D.; Eichhorn, K.-J.; Stamm, M.; Leo, K.; Riede, M. Evaluation and Control of the Orientation of Small Molecules for Strongly Absorbing Organic Thin Films. *J. Phys. Chem. C* **2013**, *117*, 11600−11609.
(37) Lunt, R. R.; Benziger, J. B.; Forrest, S. R. Relationship Between Crystalline Order and Exciton Diffusion Length in Molecular Organic Semiconductors. *Adv. Mater.* **2010**, *22*, 1233−1236.
(38) Xue, J.; Uchida, S.; Rand, B. P.; Forrest, S. R. Asymmetric Tandem Organic Photovoltaic Cells with Hybrid Planar-Mixed Molecular Heterojunctions. *Appl. Phys. Lett.* **2004**, *85*, 5757−5759.
(39) Xue, J.; Rand, B. P.; Uchida, S.; Forrest, S. R. A Hybrid Planar−Mixed Molecular Heterojunction Photovoltaic Cell. *Adv. Mater.* **2005**, *17*, 66−71.
(40) Zhou, Y.; Taima, T.; Miyadera, T.; Yamanari, T.; Kitamura, M.; Nakatsu, K.; Yoshida, Y. Phase Separation of Co-evaporated ZnPc:C60 Blend Film for Highly Efficient Organic Photovoltaics. *Appl. Phys. Lett.* **2012**, *100*, 233302.
(41) Pandey, R.; Zou, Y.; Holmes, R. J. Efficient, Bulk Heterojunction Organic Photovoltaic Cells Based on Boron Subphthalocyanine Chloride-C70. *Appl. Phys. Lett.* **2012**, *101*, 33308.
(42) Xiao, X.; Zimmerman, J. D.; Lassiter, B. E.; Bergemann, K. J.; Forrest, S. R. A Hybrid Planar-Mixed Tetraphenyldibenzoperiflanthene/C70 Photovoltaic Cell. *Appl. Phys. Lett.* **2013**, *102*, 73302.
(43) Zheng, Y-q.; Potscavage, W. J., Jr.; Komino, T.; Hirade, M.; Adachi, J.; Adachi, C. Highly Efficient Bulk Heterojunction Photovoltaic Cells Based on C70 and Tetraphenyldibenzoperiflanthene. *Appl. Phys. Lett.* **2013**, *102*, 143304.
(44) Fleetham, Tyler; O'Brien, Barry.; Mudrick, J. P.; Xue, J.; Li, J. Efficiency Enhancement in Small Molecular Organic Photovoltaic Devices Employing Dual Anode Interfacial Layers. *Proc. SPIE* **2013**, *883*, 883009.
(45) Myers, J. D.; Cao, W.; Cassidy, V.; Eom, S.-H.; Zhou, R.; Yang, L.; You, W.; Xue, J. A Universal Optical Approach to Enhancing Efficiency of Organic-Based Photovoltaic Devices. *Energy Environ. Sci.* **2012**, *5*, 6900.
(46) *Standard ASTM E973, Standard Test Method for Determination of the Spectral Mismatch Parameter between a Photovoltaic Device and a Photovoltaic Reference Cell*; American Society for Testing and Materials: West Conshocken, PA, 2002.